Hydrogen Nuclear Spin Relaxation in Hydrogen−Ice Clathrate

Lasitha Senadheera[†] and Mark S. Conradi*[,†,‡]

Departments of Physics and Chemistry, Washington University, One Brookings Drive, Saint Louis, Missouri 63130

Received: April 2, 2008; Revised Manuscript Received: May 14, 2008

H_2 in D_2O ice clathrate has been studied by hydrogen NMR. In a previous report, the H_2 line shape was shown to be due to incompletely averaged intramolecular dipolar interactions. Here the relaxation times T_1, $T_{1\rho}$, and T_2 are reported. T_1 passes through a minimum at 10 K, indicating that the rotational transition rate Γ between the three sublevels of $J = 1$ passes through the resonance frequency at this temperature. On the cold side, T_1 varies as $T^{-2.6}$; on the hot side, the rate T_1^{-1} varies as T^{-2} plus a constant (due to paramagnetic impurities). These indicate a two-phonon process drives the rotational transitions Γ. The spin-echo T_2 is nearly independent of temperature and in reasonable agreement with the Van Vleck intermolecular H_2-H_2 second moment. $T_{1\rho}$ deviates from the expected $T_{1\rho} = T_1$ behavior above 85 K, revealing an additional slow-motion source of relaxation. The deviation is driven by the hopping of H_2 between large cages. Ortho−para conversion is measured to be much slower in the clathrate than in the bulk solid, reflecting the greater distances between the H_2 molecules.

Introduction

Clathrate hydrates have icelike frameworks of H_2O molecules.[1−3] The occurrence of some pentagonal (as opposed to hexagonal) rings of H_2O molecules results in the formation of a regular array of voids, or cages. The cages can hold one or more small molecules, such as CH_4, Ar, or tetrahydrofuran (THF). In fact, in the absence of such guest molecules, the clathrate structure is not stable. A thorough review of natural gas hydrate clathrates[4] and a broader review of inclusion compounds,[5] including NMR studies,[6,7] have appeared. NMR results of classically reorienting guest molecules are well-described by broad, log−normal distributions of correlation times, reflecting the differences in the cages arising from frozen-in orientational disorder of cage-wall water molecules.[8,9] Hydrogen−ice clathrate has been recently reported and found to contain substantial[10,11] H_2. The evidence supports a type sII cubic structure, with four H_2 molecules in each large cage and only one H_2 molecule in each small cage,[12] for an overall stoichiometry of $17H_2O{\cdot}6H_2$. This amounts to a 3.77 wt % content of H_2; hydrogen clathrates thus show potential for applications in hydrogen storage.[13−15] However, a major difficulty for applications is the high pressure (>1000 bar) required for clathrate formation.[12,16] The ternary system $H_2-THF-H_2O$ forms at much lower pressure,[17,18] but holds only about 1/3 as much H_2.

To understand the basic physics of hydrogen in such cages, we have conducted hydrogen NMR studies of H_2-D_2O clathrate. In a previous paper, hereafter termed paper I, the ^1H NMR line shapes of this system were reported.[19] The dominant source of the line width is the incompletely averaged intramolecular dipole interaction. Positional disorder of D atoms in cage-wall D_2O molecules, similar to the source of residual entropy in ice Ih,[20,21] results in a different crystal field in each cage.[8,9,19] This field splits the energies of the three sublevels of the $J = 1$ ortho-H_2 molecules;[22] the unequal Boltzmann populations of the three sublevels make the time average of the intramolecular dipole interaction nonzero. We note that para-H_2 molecules have total nuclear spin $I = 0$ and so are not visible in NMR.

The line shape is controlled by the Boltzmann populations of the three sublevels; with decreasing temperature, the line broadens.[19] Down to 1.9 K, the expected full Pake powder pattern line shape[23−25] is not attained. From 12 to 120 K, the normalized line shape is essentially constant, with the *line width* varying as $1/T$. Above 120 K, further line narrowing is evident and is due to diffusion of H_2, hopping from cage to cage. Comparison with path-energetic calculations[26] suggests that the only possible hopping is between large cages, through orifices of hexagonal rings of D_2O. However, the authors of a recent paper[27] call this into question, reporting diffusion of H_2 through $H_2-TDF-D_2O$ clathrate, where the H_2 molecules are confined to the small cages only and must pass through pentagonal rings of water molecules to diffuse. In the present work we describes the spin relaxation times T_1, $T_{1\rho}$, and T_2 of H_2-D_2O clathrate, as well as ortho−para conversion.

Experimental Methods

Clathrate samples were synthesized in the beryllium−copper NMR pressure vessel[19] using high-purity H_2 gas and D_2O (99.99%). The D_2O was handled so as to minimize exposure to and exchange with atmospheric H_2O. Ground D_2O ice was held at 250 K for about 3 h under 1000−1500 bar of H_2 pressure,[16] as produced by a diaphragm compressor. The NMR vessel and sample were cooled below 77 K before release of the pressure and evacuation of excess H_2 gas not residing in the clathrate. The H_2 pressure was only used to form the clathrate, but not during NMR measurements.

The hydrogen NMR was performed at 354.2 MHz in a field of 8.32 T. The rf coil was located inside the metallic pressure vessel, at the end of an rf feedthrough.[28] Tuning and matching rf circuitries were located just above the pressure vessel, inside the cryogenic sample dewar. The pulsed spectrometer was home-

* To whom correspondence should be addressed. Office phone: (314) 935-6418. Laboratory phone: (314) 935-6292. Fax: (314) 935-6219. E-mail: msc@wuphys.wustl.edu.
† Department of Physics.
‡ Department of Chemistry.

10.1021/jp802858j CCC: $40.75
Published on Web 08/16/2008

built with a superheterodyne design. The transmitter power was typically 50 W. The signal-to-noise ratio was very high, so that little signal averaging was used. Indeed, the rate of measurement was limited primarily by the slow cooling and heating of the massive NMR pressure vessel. The rf field strength employed increased with decreasing temperature, approximately 16 kHz above 90 K, 23 kHz between 30 and 90 K, 30 kHz between 10 and 30 K, and 50 kHz between 4.2 and 10 K. For the spectra below 4.2 K, the rf pulses were 1 μs long, yielding an approximately 25° nutation angle.

The spin−lattice relaxation time T_1 was measured with the saturation−recovery−inspection strategy.[29] Saturation was accomplished by a train of 15 $\pi/2$ pulses spaced by 10 ms each; the FID following the $\pi/2$ inspection pulse was acquired. The rotating-frame spin−lattice relaxation time $T_{1\rho}$ was measured with a $(\pi/2)_X-\tau_Y$ pulse sequence, where X and Y denote rf phases.[29] The amplitude of the resulting FID was determined as a function of the spin-locking time τ. Phase cycling of the rf pulses was used.

Spin echoes using the $\pi/2-\tau-\pi/2-\tau-$echo pulse sequence were used to measure T_2. Here the second $\pi/2$ pulse serves to refocus the intramolecular H−H dipole interactions.[30] As discussed in paper I, the behaviors of *XX* and *XY* echoes are different (X and Y refer to rf phases of the two $\pi/2$ pulses).[19] All the T_2 data were taken using equal numbers of acquisitions with the *XX* and *XY* pulse phases, with appropriate phase cycling of the receiver output data to accumulate only the echo.

Ortho−para conversion[22] was studied by holding the sample at a constant temperature near 20 K and recording the NMR signal amplitude (initial amplitude following a $\pi/2$ rf pulse) over a period of 9 days. The 20 K value was chosen to be low enough that the equilibrium ortho concentration was nearly zero (0.16%), but warm enough that the consumption of liquid helium was modest. Each day or so, the sample warmed to ~40 K for ~30 min during liquid helium refilling.

Results and Discussion

At most temperatures, the signals from H_2 in the small and large cages could not be distinguished. That is, there were no data that could be taken as the sum of two distinctly different components. Thus, in the following, the analysis describes both kinds of H_2 together. An important exception is the line shapes, T_2, and $T_{1\rho}$ in the region of $T > 120$ K, where H_2 molecules diffuse between large cages.

T_1. The relaxation time data for all three samples are presented in Figure 1. The data from the different samples are very nearly the same, except as specifically remarked below. A pronounced maximum in the relaxation rate $1/T_1$ (minimum of T_1) is evident at 10 K. The asymmetry of the T_1 minimum in Figure 1 is enhanced by the log-linear graphical presentation.

Fedders' theory of nuclear spin relaxation of ortho-H_2 molecules in solid hosts[31] has been used to understand the behavior of ortho-H_2 in solid Ne, Ar, Kr, para-H_2, and amorphous hydrogenated silicon.[32,33] In the theory, transitions among the three sublevels of $J = 1$ occur at a temperature-dependent rate Γ (called Γ_2 in ref 31). These rotational-state transitions modulate the angle-dependent intramolecular dipole−dipole nuclear spin interaction,[25] resulting in nuclear spin−lattice relaxation. A characteristic feature is the predicted minimum in T_1 when Γ is approximately $1.6\omega_o$ (ω_o is 2π times the spin resonance frequency, here 354.2 MHz).

Fedders treats three cases, differing in the symmetry of the crystal field acting on the ortho-H_2 rotors.[31] The highest symmetry case leaves the three sublevels degenerate (aside from magnetic field effects) and could be used to describe fluid[34,35] H_2. The axial symmetry case leaves two out of three sublevels degenerate and describes ortho-H_2 in a solid para-H_2 host (hcp).[32] The lowest symmetry case corresponds to complete lifting of the degeneracy by unspecified crystal fields; here the spin−rotation interaction ("c" in Abragam's discussion) is quenched.[25] The predicted minimum value of T_1 occurs when $\Gamma = 1.62\omega_o$, with

$$T_1^{\min} = k\frac{\omega_0}{\omega_d^2} \qquad (1)$$

k ranges from 0.612 to 0.557, depending weakly on the value of the parameter r describing the crystal field. Here $\omega_d = 2\pi \times 57.67 \times 10^3$ rad s^{-1} expresses the magnitude of the intramolecular dipole interaction for unperturbed ortho-H_2 molecules.[31] For $\Gamma \gg \omega_o$, the dependence of T_1 is $T_1 \propto \Gamma$; for $\Gamma \ll \omega_o$, $T_1 \propto \Gamma^{-1}$.

The Pake-like spectral features[23,24] observed in H_2-D_2O clathrate[19] at 1.9 K (see paper I) reveal a cusp−cusp splitting of 164 kHz, so $\omega_d = 2\pi \times 54.7 \times 10^3$ rad s^{-1}. Not surprisingly, this value for H_2 in clathrate is very similar to that in bulk solid H_2. At our 354.2 MHz, eq 1 and this value of ω_d predict a minimum T_1 of 9.9 ms, using the middle of the narrow range of k values. The observed minimum is 24 ms. Still, the agreement is good enough to confirm that the longitudinal spin relaxation is indeed driven by transitions between the rotational sublevels, but the discrepancy is much larger than the measurement error (±5%).

One factor that can decrease the maximum *rate* $1/T_1$ is that the three sublevels of $J = 1$ are split by a large enough energy ε that their populations are unequal. That is, ε is not trivial compared to k_BT (as it is in the solidified inert gases), resulting in the observed incomplete averaging of the intramolecular

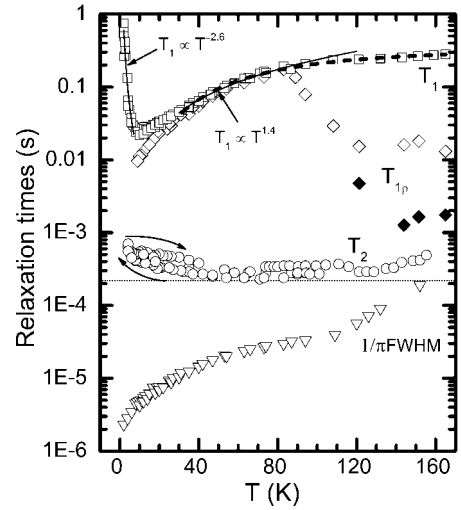

Figure 1. Relaxation times T_1 (squares), T_2 (circles), and $T_{1\rho}$ (tilted squares) and reciprocal line width ($1/\pi$(fwhm), triangles, with fwhm in hertz from ref 19) of H_2-D_2O clathrate. A characteristic T_1 minimum of 24 ms occurs at 10 K. The solid curves show that T_1 is proportional to $T^{-2.6}$ and $T^{1.4}$ on the cold side and hot side of the T_1 minimum, respectively. The dashed curve passing through the T_1 data is explained in the text. The fall of $T_{1\rho}$ at 85 K reflects cage-to-cage diffusion of H_2 guests. The filled tilted squares are $T_{1\rho}$ taken from the more slowly decaying FID component. The hysteresis behavior of T_2 at low temperatures (see arrows) indicates the effects of ortho−para conversion. The shorter (longer) T_2 data below 40 K were acquired with decreasing (increasing) temperature. The horizontal dotted line at 0.22 ms represents the calculated T_2 from intermolecular H_2-H_2 dipole interactions.

dipole interactions and the observed line width.[19] In a spectral density picture, this static (zero frequency) part of the intramolecular spin interactions reduces the strength M_2' of the *fluctuations* in this interaction which are available to drive spin−lattice relaxation.[36] Thus, we have

$$M_2' = M_2^{\mathrm{TOT}} - M_2^{\mathrm{OBSD}} \tag{2}$$

where M_2^{OBSD} is measured directly from the recorded spectrum at the temperature (10 K) of the T_1 minimum. In detail, we handle this reduction by replacing ω_d in eq 1 by ω_d' with

$$\left(\frac{\omega_d'}{\omega_d}\right)^2 = 1 - \frac{M_2^{\mathrm{OBSD}}}{M_2^{\mathrm{TOT}}} \tag{3}$$

M_2^{TOT} is calculated from the ideal Pake powder pattern of ortho-H_2 with no orientational fluctuations (see the papers by Abragam[25] and Reif and Purcell[24]). Using the result of eq 3, $\omega_d' = 2\pi \times 52.89 \times 10^3$ rad s^{-1}, so the predicted minimum T_1 is 11.8 ms from eq 1. While the effect discussed above is in the correct direction, it is not nearly large enough to explain the measured value of 24 ms.

A second way to decrease the maximum rate $1/T_1$ is for a broad distribution of rotational transition rates Γ to exist. Thus, each ortho-H_2 will pass through its own T_1 minimum at a somewhat different temperature. The result is that the *average* relaxation rate maximum is reduced. In such a scenario with a distribution of underlying T_1 values, a nonexponential magnetization recovery is expected. Indeed, our recoveries below 30 K (but not above) and more prominently at and below 10 K do depart noticeably from single exponential (the values in Figure 1 are best fits to single exponentials; we have avoided trying to further characterize those deviations, because multiexponential fits are notorious in yielding statistically uncertain decay parameters). Lorentzian relaxation peaks, such as in Fedders' theory[31] and in all BPP relaxation models,[25,37] are approximately 1 decade wide (full width at half-maximum). Thus, a *broad* distribution of rates Γ is needed to further increase the minimum T_1 to equal the observed value of 24 ms. One possible source of such a distribution is the orientational disorder of cage-wall D_2O molecules.[8,9,20,21] However, it is not clear how such static disorder would affect the phonon−rotor coupling that is responsible for Γ; our system is quite different from the classically reorienting molecules in clathrates where a broad distribution of correlation times successfully explains the data.[8,9]

We have successfully modeled the observed value of the minimum T_1 with a distribution of rates Γ spanning a range of 2.4 decades (1:256) at a given temperature. Here, we took the predicted T_1 as the reciprocal of the rate averaged across the distribution of values Γ. While we place no value in the details of our model, it does show that a very broad distribution of rates could explain the observed minimum T_1. However, the broad distribution of Γ leads to a much larger predicted ratio of T_1/T_2 (or, what is the same thing here near the T_1 minimum where the fluctuations are fast, $T_1/T_{1\rho}$) at the temperature of the T_1 minimum. We observe a ratio $T_1/T_{1\rho}$ of about 2.2, close to the value that Fedders' theory[31] predicts (T_1/T_2 at the T_1 minimum is 1.6) for a single Γ. The broad distribution that fits the observed minimum T_1 predicts a T_1/T_2 of about 5.6. We conclude that we have no satisfactory picture capable of explaining the observed minimum value of T_1 *and* that is consistent with the behavior of $T_{1\rho}$ in Figure 1.

Our rf field strength (see the Experimental Methods) was somewhat weak, given the broad lines observed here. Can this explain the observed minimum T_1? The weak rf field will tend to lead to effective saturation at the center of the resonance and less saturation in the wings. The central portion of the line can then recover either by true T_1 processes or by spectral diffusion (carried by H_2−H_2 intermolecular dipole interactions). Thus, the signal would recover faster, leading to a decreased value of the minimum T_1. This is in the opposite sense to the observed discrepancy, so this effect cannot explain the discrepancy between the measured and calculated minimum T_1 values.

In connection with this, we note that, at low temperatures where the resonance is broadest, the intermolecular H_2−H_2 dipole interactions (see T_2 in Figure 1) are weakest compared to the line width (see $1/\pi$(fwhm) in Figure 1). Thus, intermolecular spin flip-flops (spin diffusion) should be slower at low temperatures than at high temperatures, because the intermolecular interactions are much smaller (at low T) than typical intramolecular dipole energy mismatches. In general, the large intramolecular broadening reduces the rate of intermolecular spin flip-flops.

On the warm side of the T_1 minimum, from 30 to 100 K, T_1 varies approximately as $T^{1.4}$; on the cold side from 2 to 7 K, the variation follows $T_1 \propto T^{-2.6}$. These dependences appear in Figure 1 as solid lines through the data. By analogy with ortho-H_2 in the solidified rare gases[32] and in amorphous hydrogenated silicon,[33] one expects Γ to be driven by two-phonon relaxation, as discussed by van Krandendonk.[38,39] At high temperature, this should lead to $\Gamma \propto T^2$ (so $T_1 \propto T^2$ on the hot side of the minimum) and $\Gamma \propto T^n$ at low temperatures (with $2 \leq n \leq 7$, so $T_1 \propto T^{-n}$ on the cold side). Our results are broadly in agreement with these predictions.

We note that T_1 becomes more nearly independent of temperature above 80 K; we believe this is due to the presence of paramagnetic impurities,[40] probably oxygen introduced by the D_2O ice used to prepare the clathrate. Another possible source of paramagnetic relaxation centers is the damage in the D_2O occurring during grinding at low temperature (we thank an anonymous reviewer for this suggestion). We can successfully fit the T_1 data above 30 K with an intrinsic T_1 varying as T^2 and a constant T_1 from impurities:

$$\left(\frac{1}{T_1}\right)^{\mathrm{OBSD}} = \frac{1}{aT^2} + \frac{1}{b} \tag{4}$$

where $b = 0.35$ s. The fit using eq 4 appears in Figure 1 as a dashed curve. It fits the data over a wider range of temperature than the solid curve representing $T^{1.4}$, demonstrating that the highest temperature measurements of T_1 are indeed reduced by paramagnetic impurities. The underlying T^2 variation in eq 4 also is in better accord with expectations for relaxation driven by two-phonon processes.

T_2. Spin echoes were used to measure the decay time T_2, as reported in Figure 1. What interactions control T_2? The intramolecular dipole interaction has static parts which dominate the observed line width; these are refocused by the $\pi/2-\tau-\pi/2$ pulse sequence, as discussed in paper I, so they do not contribute to the echo T_2. The fluctuating parts of the intramolecular dipole interaction fluctuate at the molecular rotation transition rate Γ and control T_1. At temperatures at and above 10 K, the T_2 from this process should be approximately equal to T_1 (see the $T_{1\rho}$ data in Figure 1); this measured rate $1/T_{1\rho}$ is entirely negligible compared to the measured decay rate $1/T_2$. Deuteron nuclear spins from cage-wall D_2O molecules are in dipolar interaction with the ortho-H_2. These *unlike-spin* interactions[25] are refocused by the second pulse, so they also do not lead to T_2 decay of the echo envelope.

Intermolecular dipolar interactions between ortho-H_2 molecules *do* result in T_2 decay. At the simplest level, the second rf pulse flips the spins in both molecules, so the intermolecular interaction is not time-reversed. As noted earlier, the H_2-H_2 interactions are not expected to result in rapid spin flip-flops, because of the larger intramolecular interactions. Thus, most of the T_2 decay from intermolecular H_2-H_2 interaction should be explained by the A terms ($I_{Z_1}I_{Z_2}$) of this interaction.[41]

The positions of the cage centers are known[2,12,42] and were used to calculate the powder average Van Vleck second moment M_2^{INTER}, using only the A terms.[25,41,43] This is

$$M_2^{\mathrm{INTER}} = c\frac{4}{15}\gamma^4\hbar^2 I(I+1)\sum_k \frac{1}{r_k^{\,6}} \qquad (5)$$

where $I = 1$ for an ortho-H_2 and c is the fractional ortho concentration, taken here as $c = 0.5$, the equilibrium concentration[22] at 80 K. Each small cage had one H_2 molecule, and each large cage was given four[12] H_2 molecules. The intermolecular interactions within each large cage were assumed to average to zero, by virtue of translations (rolling) of the four molecules inside each cage (but see below). The result is $M_2^{\mathrm{INTER}} = 43.2 \times 10^6$ rad^2 s^{-2}. Assuming a Gaussian line shape for simplicity, this corresponds to a Gaussian echo decay with a T_2 (the $1/e$ time) of 0.22 ms, in reasonable accord with the data. This value appears as a dotted line in Figure 1.

The discrepancy (larger measured T_2 than predicted) may indicate that the ortho-fractional concentration c was less than 0.5. Also, ortho−para conversion is expected to lead to anticlustering of the ortho-H_2, as regions of high ortho density tend to convert more rapidly. The linear factor of c in eq 5 is exact for *random dilution*;[25] if anticlustering occurs, eq 5 overestimates M_2^{INTER} and underestimates the echo decay time T_2. Finally, we note that our echo envelope decays were well described by

$$E(\tau) = A\exp[-(2\tau/T_2)^n] \qquad (6)$$

with the parameter n typically equal to 1.4 ± 0.1 over most of the decay. This value of n is smaller than 2 (the Gaussian case), which results in a "line shape" with a smaller fwhm and longer T_2 for a given M_2^{INTER}. In any event, the approximate agreement between the observed echo T_2 and the calculated M_2^{INTER} suggests that we have correctly identified the source of the echo envelope decay.

There were variations in T_2 within individual samples and between different samples. We believe these are due to ortho−para conversion (and reconversion at high temperatures). We note the arrows on the T_2 data in Figure 1, showing the direction of temperature change (recall the large thermal mass dictated that change from 80 to 20 K might occur over 1 or more days). The lower T_2 taken upon cooling is in accord with a slightly larger ortho concentration, from presumed reconversion during the immediately prior time spent at high temperature. The data taken upon subsequent warming are expected to have a slightly smaller ortho concentration, explaining the slightly longer observed T_2.

Because the symmetry of each large cage is lower than the ideal tetrahedral symmetry due to D_2O orientational disorder,[8,9,19,44] the intermolecular dipole interactions of the H_2 molecules within a single large cage may not time-average to zero. In the absence of a way to calculate this effect, we note this would only increase M_2^{INTER} and decrease the predicted T_2. As the predicted T_2 already is slightly below the measured value from spin echoes, this effect must be small or zero.

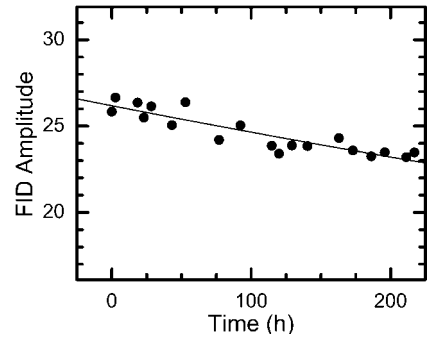

Figure 2. Evidence of ortho−para conversion of H_2 guest molecules in H_2-D_2O clathrate. FID amplitudes are measured at ~20 K over 217 h. The FID signal amplitudes shown above are corrected for temperature variation during the experiment. The estimated second-order (k_2) and first-order (k_1) conversion rate constants are $k_2 = 13 \times 10^{-4}$ h^{-1} and $k_1 = 6 \times 10^{-4}$ h^{-1}. The solid curve is the approximate fitting to the first-order decay; the second-order fitting curve is nearly indistinguishable.

Ortho−Para Conversion. Conversion measurements were made on sample 2, by holding it at 20 K for 217 h. This sample had been synthesized 42 days earlier, with temperature variation from 2 to 94 K. The NMR signal amplitude (initial value of FID, following a $\pi/2$ pulse) was recorded. Small changes in the measurement temperature (less than ± 1 K) were handled by correcting for the anticipated $1/T$ Curie spin susceptibility.

The signal amplitude data, so corrected, are displayed in Figure 2. The fractional changes are small, indicating that ortho−para conversion is slow here. If the conversion follows second-order kinetics as in bulk H_2 (o + o ↔ o + p)[22,45]

$$\frac{dc}{dt} = -k_2 c(c - c_{\mathrm{eq}}) \approx -k_2 c^2 \qquad (7)$$

where the approximation is good at low temperatures such as 20 K, where $c_{\mathrm{eq}} \approx 0$. However, the H_2 molecules in H_2-D_2O clathrate are well-separated, and the conversion rate from the above mechanism is a strong function of the intermolecular distance (about R^{-12}), depending on the details of the phonon spectrum.[22,46] Thus, the second-order mechanism *may* be negligible compared to first-order conversion driven by dipole interaction between deuterium nuclei and H_2 (D + o ↔ D + p):

$$\frac{dc}{dt} = -k_1(c - c_{\mathrm{eq}}) \approx -k_1 c \qquad (8)$$

The curve through the data of Figure 2 corresponds to eq 8 with $k_1 = 6 \times 10^{-4}$ h^{-1}; the deviation from a straight line is negligible over this small extent of conversion. The same curve nearly describes second-order conversion, eq 7, with $k_2 = 13 \times 10^{-4}$ h^{-1} (assuming the initial concentration during the 217 h interval was 0.5, on the basis of the temperature history). We note the conversion in bulk solid H_2 is *much* faster,[22] with $k_2 = 190 \times 10^{-4}$ h^{-1}. The present samples have paramagnetic relaxation centers (probably O_2), according to the high-temperature T_1 data, as discussed above. These may contribute to ortho−para conversion, so the small, measured value should be regarded as an upper limit on the intrinsic conversion rate.

In short, conversion is very slow in the clathrate, in accord with the large spacing between cages. However, there are four H_2 molecules in each large cage. It seems to us one would expect a bulklike rate of conversion for the three ortho-H_2 molecules initially (on average) residing in the large cage. Possibly the conversion of these down to one ortho-H_2 molecule (where this

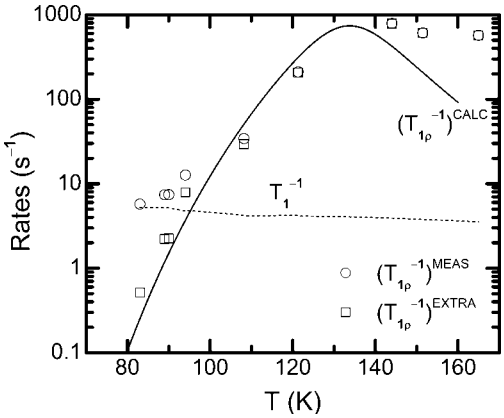

Figure 3. Relaxation rates in the rotating frame at $T > 80$ K. The solid curve represents the calculated rate $(T_{1\rho}^{-1})^{CALCD}$ due to diffusion from eq 10. The extra contribution to the $T_{1\rho}$ relaxation, $(T_{1\rho}^{-1})^{EXTRA}$, is denoted by squares and is the difference of the measured $(T_{1\rho}^{-1})^{MEASD}$ (circles) and the laboratory-frame T_1^{-1} (dotted line) using the relationship in eq 9.

mechanism would be completed) occurs rapidly, so it does not appear in the data of Figure 2. Indeed, at high temperatures where the signals of H_2 in small and large cages can be separated, it appears the fraction of ortho-H_2 in large cages (out of the total ortho-H_2 molecules) is small (see below).

***$T_{1\rho}$* and H_2 Diffusion.** The measured values of $T_{1\rho}$ in Figure 1 between 8 and 85 K behave qualitatively as expected from BPP relaxation theory.[37] That is, well above the T_1 minimum where the molecular rotational transition rate Γ obeys $\Gamma \gg \omega_o$, $T_{1\rho}$ and T_1 are nearly equal. As the T_1 minimum is approached from above, $T_{1\rho}$ becomes less than T_1. For temperatures below 8 K, the line is so broad that our rf field strength is inadequate to perform a good spin lock. There, the signals obtained after the spin-locking rf pulse have mixed Zeeman and dipolar character, making analysis difficult. For this reason, only $T_{1\rho}$ data above 8 K appear in Figure 1.

At $T > 120$ K, the NMR line narrows as reported in paper I and as shown as $1/\pi$(fwhm) in Figure 1. On the basis of calculations of the energy[26] (5−6 kcal/mol) for a H_2 to pass through a hexagonal ring of D_2O molecules separating neighboring large cages, the line narrowing has been assigned to H_2 in large cages only. By comparison, the energy to pass through the pentagonal rings separating small cages from each other (or small cages from large ones) is about 5 times larger, making this path unlikely. However, we note a recent report[27] of H_2 diffusion measured by pulsed field gradient NMR in H_2−TDF−D_2O clathrate, which is very similar to H_2−D_2O except that the H_2 molecules are confined to the small cages only. Remarkably, the measured activation energy[27] is only 0.7 kcal/mol, much smaller than the calculated ∼26 kcal/mol.

Above 120 K, the NMR spectrum can be readily resolved as a superposition of a broad line (from the more rapidly decaying component of the FID, assigned to H_2 in small cages) and a narrow line (from the slowly decaying part of the FID, assigned to H_2 in large cages) as appears at the top of Figure 1 of paper I. By comparing the areas of the two spectral components (or the initial amplitudes of the FID components), the fractions of ortho-H_2 molecules in each environment were obtained (recall para-H_2 has no NMR signal). We find that only approximately 1/4 to 1/3 of all the ortho-H_2 molecules in the sample at 130−152 K reside in large cages. We note that, while less than half of the spectral area is from H_2 in large cages at these temperatures, the spectral peak height and the fwhm as reported in paper I and in Figure 1 reflect primarily the narrow resonance from these large-cage H_2 molecules. By comparison, if every large cage were occupied by four H_2 molecules, 2/3 of all the H_2 molecules (not distinguishing ortho and para) would be in large cages. Lokshin et al. have shown from their neutron diffraction study[12] that the average occupancy of the large cages decreases from 4 at 80 K and below to about 2 near 160 K; the occupation of small cages remains near 1. This is a kinetic effect, with the H_2 molecules leaving the clathrate into the surrounding near vacuum. With only two H_2 molecules per large cage, 1/2 of all the H_2 molecules remaining are in large cages. We note that the decreasing average occupation by H_2 of the large cages should virtually eliminate site-blocking effects; most large cages will be able to receive an additional H_2 molecules.

Thus, it appears that, regardless of the extent of large-cage occupation between 2 and 4, the finding of only 1/4 to 1/3 of all the ortho-H_2 molecules residing in large cages implies that the large-cage H_2 molecules have been *preferentially* converted to para-H_2. The close proximity of the H_2 molecules to each other in large cages is a possible mechanism for this, as discussed above.

We monitored the total ortho-H_2 content of a clathrate sample by measuring the initial amplitudes of FIDs after $\pi/2$ rf pulses. Between 53 and 87 K, spanning a 27 h period, the signal amplitude (corrected for the $1/T$ dependence of Curie's law) was constant to within ±2%, confirming that H_2 does not leave the sample at these temperatures. After a subsequent 7 days spent below 20 K, the corrected signal at 94 K had decreased by about 12%, in approximate accord with the ortho−para conversion rate evident in the data of Figure 2. The sample was then warmed over 24 h to 109 K, losing 7% of its signal. In the next 24 h, the temperature was increased from 109 to 164 K and the signal decreased (steadily) by 44%. Clearly, at the high temperatures (but not at or below 87 K), H_2 was evaporating from the sample into the surrounding vacuum. A further increase of temperature resulted in nearly complete NMR signal loss, indicating decomposition of the clathrate.

With H_2 molecules in large cages diffusing and undergoing large changes in their intramolecular dipole interactions, one would expect the echo-derived T_2 to first decrease (in the slow motion limit of mean time between jumps times frequency changes much greater than 1) and then increase in the motional averaging regime. For example, such behavior appears in the echo T_2 data of α-CO,[47] CO_2,[48] and in TDF−H_2O clathrate (above 140 K in Figure in ref 44). However, the FID initial amplitude and spin-echo peak amplitude *here* primarily reflect the behavior of H_2 in small cages (recall the signal from H_2 in large cages is only 1/4 to 1/3 of the total). Thus, the T_2 data in Figure 1 show only a very weak decrease near 120 K. The weak increase of T_2 at yet higher temperatures should reflect the decreased H_2 occupancy of large cages (and the resulting decrease in M_2^{INTER}) and the motional averaging of intermolecular dipole interactions between H_2 molecules in small and large cages.

At temperatures at and above 120 K, $T_{1\rho}$ was analyzed in two ways. The open tilted squares in Figure 1 were obtained by measuring the *initial* amplitude of the FID following each spin-locking pulse. This equally weights the ortho-H_2 molecules regardless of their location in small or large cages. The filled tilted squares in Figure 1 were obtained by measuring the amplitude of only the slowly decaying part of the FID (hence, H_2 in large cages). This separation is relatively clean at the three highest temperatures where the line narrowing is prominent; at 120 K, the two components are harder to resolve. The result is

that the H_2 molecules in large cages (filled tilted squares) show a much deeper decrease in $T_{1\rho}$, because they are the mobile species undergoing intramolecular-frequency changes.

Thus, the appearance of pronounced line narrowing is consistent with the T_2 data and the $T_{1\rho}$ data. However, we note that the *assignment* of the narrow line to H_2 in large cages rests upon the calculations[26] of the energy barriers for H_2 to pass through hexagonal or pentagonal rings of D_2O molecules. Measurements of H_2 in $H_2-TDF-D_2O$ (in preparation for publication) confirm this assignment.

Above 85 K, $T_{1\rho}$ decreases sharply, no longer following closely the values of T_1. We assert that the measured rate is the sum of T_1^{-1} and some extra contribution due to diffusion, $(T_{1\rho}^{-1})^{\mathrm{EXTRA}}$:

$$(T_{1\rho}^{-1})^{\mathrm{MEASD}} = T_1^{-1} + (T_{1\rho}^{-1})^{\mathrm{EXTRA}} \quad (9)$$

In Figure 3, the data are treated accordingly to show the extra contribution $(T_{1\rho}^{-1})^{\mathrm{EXTRA}}$ as squares. Clearly, the extra relaxation reflects a slow motion which only becomes rapid enough above 85 K to be evident above the background, T_1^{-1}. For $T \geq 120$ K, the $T_{1\rho}$ values from the long part of the FIDs (filled tilted squares in Figure 1) were used.

Cage-to-cage hopping (diffusion) will contribute to $T_{1\rho}^{-1}$. This contribution will be[49]

$$(T_{1\rho}^{-1})^{\mathrm{CALCD}} = M_2\left(\frac{\tau}{1+4\omega_1^2\tau^2}\right) \quad (10)$$

where M_2 is to be taken from the *observed* line shape at each temperature. That is, diffusion modulates only that portion of the intramolecular interaction remaining after rapid averaging[44] by the rotational transitions at Γ. In practice the second moment M_2 was taken from the recorded line shapes below 120 K; above 120 K, where the line is motionally narrowed, a simple $1/T^2$ extrapolation of the lower temperature M_2 values was used. The correlation time τ is related to the diffusive hopping rate ω_H, with $\tau = 1/\omega_H$. Here ω_1 is the angular frequency of nutation of the spin-lock pulse, 2π times 16 kHz at the relevant temperatures. The predicted contribution $(T_{1\rho}^{-1})^{\mathrm{CALCD}}$ using eq 10 appears in Figure 3 as the solid curve. The parameters to describe $\omega_H = 1/\tau$ were an attempt frequency of 10^{12} s^{-1} and an activation energy of 4.1 kcal/mol, nearly the same parameters determined from the onset of line narrowing in paper I (10^{12} s^{-1} and 3.8 kcal/mol).[19] The calculated contribution to $T_{1\rho}^{-1}$ does a reasonable job of explaining the extra part of the measured $T_{1\rho}^{-1}$, given the uncertainties in the assumptions about M_2 and ω_H while this system is decomposing.

Conclusions

Spin−lattice relaxation of ortho-H_2 in H_2-D_2O clathrate is driven by transitions at rate Γ among the three sublevels of the $J = 1$ rotational state. A T_1 minimum is observed at 10 K, indicating that Γ passes approximately through the resonance frequency. The temperature dependence of T_1 is consistent with transitions at rate Γ being driven by two-phonon processes. At high temperatures, T_1 appears to be limited by paramagnetic (likely O_2) impurities serving as relaxation centers. The value of T_1 at the minimum is larger than predicted; attempts to fit the minimum by invoking a distribution of rates Γ yield values of $T_1/T_{1\rho}$ at 10 K that are too large.

The echo decay time constant T_2 results from H_2-H_2 intermolecular dipole interactions. The measured T_2 varies only weakly with temperature and is in reasonable accord with the value from the Van Vleck lattice sum and calculated M_2^{INTER}. Small changes and hysteresis in T_2 upon temperature cycling are in qualitative agreement with the expected effects of ortho−para conversion.

Ortho−para conversion in H_2-D_2O clathrate is slow. The result from a 217 h measurement at 20 K is $k_1 = 6 \times 10^{-4}$ h^{-1} (first-order conversion) or $k_2 = 13 \times 10^{-4}$ h^{-1} (second-order conversion), much smaller than the conversion in bulk solid, $k_2 = 190 \times 10^{-4}$ h^{-1}. The slower conversion qualitatively agrees with the much greater H_2-H_2 distances in the clathrate.

The rotating-frame spin−lattice relaxation time $T_{1\rho}$ is nearly equal to T_1 from 25 to 85 K, as expected for $\Gamma \gg \omega_o$. Above 85 K, an additional relaxation contribution is evident from the rapid decrease in $T_{1\rho}$. The additional relaxation agrees with the calculated relaxation based on the rate of H_2 hopping between large cages, as determined in paper I through line narrowing. Above 120 K, two-component FIDs are interpreted as nondiffusing H_2 in small cages (rapidly decaying FID) and rapidly diffusing H_2 in large cages (slowly decaying FID). This decomposition is confirmed by the $T_{1\rho}$ measurements, which find a much more rapid decay rate $T_{1\rho}^{-1}$ of the long part of the FID (from the diffusing species).

Acknowledgment. We acknowledge financial support through NFS Grant DMR-0400512. L.S. appreciates support from the Washington University through a dissertation fellowship. We appreciate the input of two anonymous reviewers.

References and Notes

(1) Englezos, P. *Ind. Eng. Chem. Res.* **1993**, *32*, 1251.
(2) Sloan, E. D. *Clathrate Hydrates of Natural Gases*, 2nd ed.; Marcel Dekker: New York, 1998.
(3) Mao, W. L.; Koh, C. A.; Sloan, E. D. *Phys. Today* **2007**, *60*, 42.
(4) Koh, C. A. *Chem. Soc. Rev.* **2002**, *31*, 157.
(5) Atwood, J. L.; Davies, J. E. D.; MacNicol, D. D. *Inclusion Compounds: Physical Properties and Applications*; Academic Press: Orlando, FL, 1984; Vol. 3.
(6) Davidson, D. W.; Ripmeester, J. A. *J. Glaciol.* **1978**, *21*, 33.
(7) Davidson, D. W.; Ripmeester, J. A. NMR, NQR and Dielectric Properties of Clathrates. In *Inclusion Compounds*; Atwood, J. L., Davies, J. E. D., MacNicol, D. D., Eds.; Academic Press: Orlando FL, 1984; Vol. 3, p 69.
(8) Garg, S. K.; Davidson, D. W.; Ripmeester, J. A. *J. Magn. Reson.* **1974**, *15*, 295.
(9) Ripmeester, J. A.; Ratcliffe, C. I.; Cameron, I. G. *J. Phys. Chem. B* **2004**, *108*, 929.
(10) Mao, W. L.; Mao, H. K.; Goncharov, A. F.; Struzhkin, V. V.; Guo, Q. Z.; Hu, J. Z.; Shu, J. F.; Hemley, R. J.; Somayazulu, M.; Zhao, Y. S. *Science* **2002**, *297*, 2247.
(11) Mao, W. L.; Mao, H. K. *Proc. Natl. Acad. Sci. U.S.A.* **2004**, *101*, 708.
(12) Lokshin, K. A.; Zhao, Y. S.; He, D. W.; Mao, W. L.; Mao, H. K.; Hemley, R. J.; Lobanov, M. V.; Greenblatt, M. *Phys. Rev. Lett.* **2004**, *93*, 125503.
(13) Strobel, T. A.; Koh, C. A.; Sloan, E. D. *Fluid Phase Equilib.* **2007**, *261*, 382.
(14) Manakov, A. Y.; Skiba, S. S. *Russ. J. Gen. Chem.* **2007**, *77*, 740.
(15) Struzhkin, V. V.; Militzer, B.; Mao, W. L.; Mao, H. K.; Hemley, R. J. *Chem. Rev.* **2007**, *107*, 4133.
(16) Lokshin, K. A.; Zhao, Y. S. *Appl. Phys. Lett.* **2006**, *88*, 131909.
(17) Florusse, L. J.; Peters, C. J.; Schoonman, J.; Hester, K. C.; Koh, C. A.; Dec, S. F.; Marsh, K. N.; Sloan, E. D. *Science* **2004**, *306*, 469.
(18) Strobel, T. A.; Taylor, C. J.; Hester, K. C.; Dec, S. F.; Koh, C. A.; Miller, K. T.; Sloan, E. D. *J. Phys. Chem. B* **2006**, *110*, 17121.
(19) Senadheera, L.; Conradi, M. S. *J. Phys. Chem. B* **2007**, *111*, 12097.
(20) Fletcher, N. H. *The Chemical Physics of Ice*; Cambridge University Press: London, 1970.
(21) Hobbs, P. V. *Ice Physics*; Oxford University Press: London, 1974.
(22) Silvera, I. F. *Rev. Mod. Phys.* **1980**, *52*, 393.
(23) Pake, G. E. *J. Chem. Phys.* **1948**, *16*, 327.
(24) Reif, F.; Purcell, E. M. *Phys. Rev.* **1953**, *91*, 631.
(25) Abragam, A. *The Principles of Nuclear Magnetism*; Clarendon Press: London, 1961.
(26) Alavi, S.; Ripmeester, J. A. *Angew. Chem., Int. Ed.* **2007**, *46*, 6102.
(27) Okuchi, T.; Moudrakovski, I. L.; Ripmeester, J. A. *Appl. Phys. Lett.* **2007**, *91*, 171903.

(28) Schouten, J. A.; Trappeniers, N. J.; Goedegebuure, W. *Rev. Sci. Instrum.* **1979**, *50*, 1652.

(29) Fukushima, E.; Roeder, S. B. W. *Experimental Pulse NMR: a Nut and Bolt Approach*; Addison-Wesley: Reading, MA, 1981.

(30) Yu, I.; Washburn, S.; Meyer, H. *J. Low Temp. Phys.* **1983**, *51*, 369.

(31) Fedders, P. A. *Phys. Rev. B* **1979**, *20*, 2588.

(32) Conradi, M. S.; Luszczynski, K.; Norberg, R. E. *Phys. Rev. B* **1979**, *20*, 2594.

(33) Conradi, M. S.; Norberg, R. E. *Phys. Rev. B* **1981**, *24*, 2285.

(34) Hardy, W. N. *Can. J. Phys.* **1966**, *44*, 265.

(35) Lipsicas, M.; Hartland, A. *Phys. Rev.* **1963**, *131*, 1187.

(36) Conradi, M. S. *Phys. Rev. B* **1983**, *28*, 2848.

(37) Bloembergen, N.; Purcell, E. M.; Pound, R. V. *Phys. Rev.* **1948**, *73*, 679.

(38) Kranendonk, J. V. *Physica* **1954**, *20*, 781.

(39) Kranendonk, J. V.; Walker, M. B. *Can. J. Phys.* **1968**, *46*, 2441.

(40) Ripmeester, J. A.; Garg, S. K.; Davidson, D. W. *J. Magn. Reson.* **1980**, *38*, 537.

(41) Slichter, C. P. *Principles of Magnetic Resonance*, 3rd ed.; Springer: New York, 1996.

(42) Mark, T. C. W.; McMullan, R. K. *J. Chem. Phys.* **1965**, *42*, 2732.

(43) Van Vleck, J. H. *Phys. Rev.* **1948**, *74*, 1168.

(44) Davidson, D. W.; Garg, S. K.; Ripmeester, J. A. *J. Magn. Reson.* **1978**, *31*, 399.

(45) Kranendonk, J. V. *Solid Hydrogen: Theory of the Properties of Solid H2, HD, and D2*; Plenum Press: New York, 1983.

(46) Berlinsky, A. J.; Hardy, W. N. *Phys. Rev. B* **1973**, *8*, 5013.

(47) Liu, S.-B.; Conradi, M. S. *Phys. Rev. B* **1984**, *30*, 24.

(48) Liu, S.-B.; Doverspike, M. A.; Conradi, M. S. *J. Chem. Phys.* **1984**, *81*, 6064.

(49) Boden, N. NMR Studies of Plastic Crystals. In *The Plastically Crystalline State*; Sherwood, J. N., Ed.; John Wiley and Sons: Chichester, U.K., 1979; p 147.

JP802858J